Yijun Qiao
College of Mechanical and Vehicle Engineering,
Taiyuan University of Technology,
Taiyuan 030024, China
e-mail: 13513603599@163.com

Yun-Bo Yi
Department of Mechanical and
Materials Engineering,
University of Denver,
Denver, CO 80208
e-mail: Yun-Bo.Yi@du.edu

Tie Wang[1]
College of Mechanical and Vehicle Engineering,
Taiyuan University of Technology,
Taiyuan 030024, China
e-mail: wangtie57@163.com

Hongwei Cui
College of Mechanical and Vehicle Engineering,
Taiyuan University of Technology,
Taiyuan 030024, China;
The State Key Laboratory of Mechanical
Transmissions,
Chongqing University,
Chongqing 400044, China
e-mail: cuihongwei@tyut.edu.cn

Zisheng Lian
College of Mechanical and Vehicle Engineering,
Taiyuan University of Technology,
Taiyuan 030024, China
e-mail: lianzisheng@tyut.edu.cn

Effect of Wear on Thermoelastic Instability Involving Friction Pair Thickness in Automotive Clutches

Wear is an inevitable phenomenon in the working process of clutch and brake system. With the increase of transmission speed and power density, the thermoelastic instability (TEI) of clutch and brake system is becoming more serious over time. It is difficult to obtain the practical solution for conventional materials of clutches and brakes and their actual geometry with finite thickness using the existing analytical method. To study the comprehensive effects of wear and friction pair thickness on TEI, Archard Wear Law is combined with the Fourier Reduction Method to develop a finite element model, the accuracy of which is validated using the existing analytical method. Within the usual ranges of thickness and wear coefficient of friction pair, the increase of friction material thickness or the decrease of steel material thickness will suppress the TEI. Nonetheless, if the wear-rate is increased significantly, the effect of friction material thickness will be reversed. The worst thickness, which must be avoided in the design, and the local optimum thickness exist for the steel material.
[DOI: 10.1115/1.4052781]

Keywords: clutches, hotspots, thermoelastic instability, wear

1 Introduction

The clutches and brakes, which usually include one or more friction pairs, are the key components of mechanical transmission. As the speed and power density increase, the transmission system puts forward higher requirements on the performance and service life of clutches and brakes. For instance, as shown in Fig. 1, the hydro-viscous clutch is composed of multiple sets of friction discs and separator discs. The friction pair gap is filled with working oil, and the torque and power are transmitted through this oil film shearing and friction. It supports soft start, stepless speed regulation, overload protection, and high reliability [1,2]. Local ablation of friction discs, warping and cracking of steel discs often lead to clutch failure, and brake systems often pulsate due to uneven torque at the brake pad/rotor interface, known as hot judder [3]. The causes of these phenomena are as follows: during friction pair sliding, a large amount of mechanical energy is converted into internal energy. This leads to a high surface temperature of friction pair and large temperature difference of friction material, resulting in large thermal stress. The friction side will degrade or fail if the temperature or thermal stress exceeds the allowable limit of the material. On the other hand, there is some initial non-uniformity of the physical field inside the friction pair because of manufacturing error, installation issue, structure mismatch, control error, etc. Frictionally excited thermoelastic instability (TEI) will occur if the sliding speed of the friction pair exceeds the critical value [4]. The inhomogeneity of the initial physical field will increase exponentially with time, leading to local high-temperature regions on the surface of the friction pair, which will damage the friction surface. This will result in performance degradation or failure of the transmission system [5].

Barber [4] first made a theoretical study on TEI and figured out that when sliding friction occurs between two solids, the irregularity of the surface will result in the non-uniform distribution of contact pressure, then causing the non-uniform distribution of friction heat and thermal expansion of the material, exaggerating the initial irregularity of the surface. The friction heat will be concentrated in the high-pressure region, resulting in local hot spots. A theoretical model for the sliding of the blade and the semi-infinite plane was established by Dow and Burton [6], focusing on the study of the

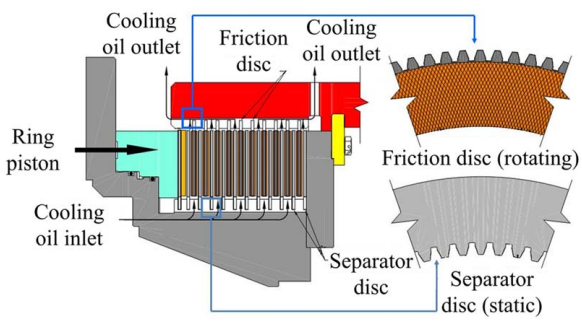

Fig. 1 Structure of the hydro-viscous clutch

[1]Corresponding author.

Contributed by the Tribology Division of ASME for publication in the JOURNAL OF TRIBOLOGY. Manuscript received September 17, 2021; final manuscript received October 15, 2021; published online November 12, 2021. Assoc. Editor: Yong Hoon Jang.

TEI problem of the system by a perturbation method. They figured out that if the sliding speed exceeds the critical value, the initial disturbance will boost exponentially in the system, and the system would become unstable. Burton et al. [7] studied the two limiting cases: friction pair composed of the same material, or heat conductor slide on thermal insulation, concluding that the latter system is more prone to TEI, whereas it occurs only with a bigger friction coefficient for the first friction system. Considering the lubricant, Jang and Khonsari [8] developed a conductor-insulator model and identified the elongated hotspots when the sliding speed of the friction pair was much higher than migration speed. Lee and Barber [5] presented a solution to the TEI problem involving steel material thickness, providing a reliable prediction of the critical velocity and TEI mode of the typical brake assembly. This is widely used in TEI analysis in the brake and clutch industry.

Thermoelastic instability problems are usually solved using the Finite element method. Yi et al. [9] developed the Fourier reduction method to solve the TEI problems, which can compute the critical velocity and the exponential growth rate of the system when sliding above the critical velocity. Besides, Yi [10] built the finite element model of the thermoelastodynamic instability (TEDI) problem, the coupling effect of the dynamic and thermoelastic instability, proposed the solution method for the high order eigenvalue equations, and predicted growing modes at a lower speed than the critical speed. Another type of friction-induced instability caused by the temperature-dependent coefficient of friction was studied by Mortazavi et al. [11]. Zagrodzki and Macey [12] studied the transient thermoelastic issue of clutches and brakes by combining the simulation and test results, concluding the suitability of the plane strain model for the TEI problem. Zagrodzki [13] also developed the TEI transient model by finite element method and modal superposition, demonstrating that most of the actualized clutches operate above the critical speed. The finite element solution of the TEI eigenvalue problem with coarse discretization in the time domain was studied by Abdullah and AL-Shabibi [14]. This significantly improved the computational efficiency of the transient TEI model.

Certain studies are conducted on the effects of wear on TEI. In early 1969, when the concept of TEI was first proposed, Barber [4] came up with some experimental research to reveal the complexity of the relationship between wear and TEI. Dow and Burton [15] introduced the influence of wear on the theoretical model of a blade pressed against the above-mentioned semi-infinite plane and concluded that wear would inhibit the TEI. Papanglo and Ciavarella [16,17] showed that the wear would reduce the stability of the system in some cases and stated a critical wear-rate, beyond which the TEI will be completely suppressed for the nonconducting half-space model. The finite element method was introduced by Qiao et al. [18] to study the influence of wear on TEI, by which, however, only the models with very thick materials were studied, without considering the effects of thickness reduction on the result.

Owing to the complexity of geometry and the particularity of the commonly used materials, the analytical method has limitations of a few simple cases. In this study, the finite element method is used to solve the TEI problem of practical brakes or clutches. The Archard wear law is introduced into the Fourier reduction method, the two-dimensional friction sliding model of the bi-material interface is applied, and the graded mesh method is used to capture the drastically changing temperature and stress on the contact surface, so the combined effects of wear and material thickness on TEI could be studied.

2 Method

2.1 Finite Element Method. A two-dimensional sliding system is considered, in which a moving body (material 1) slides on a stationary body (material 2) in the positive x direction with a constant velocity V. The two bodies touch on a common interface

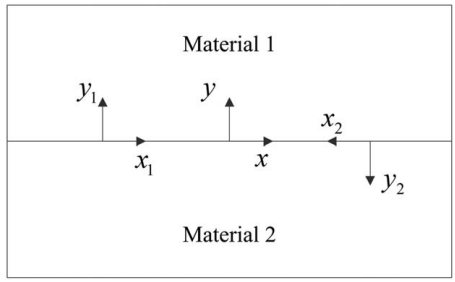

Fig. 2 Schematic of two sliding materials

(Fig. 2), assuming that all the boundaries except the sliding interface are adiabatic, and the two objects extend indefinitely in the horizontal x direction.

2.1.1 Temperature Field. The heat conduction equation is as follows:

$$K_i \nabla^2 T - \rho_i c_{pi}\left(\frac{\partial T}{\partial t} + V\frac{\partial T}{\partial x}\right) = 0 \tag{1}$$

where K_i, ρ_i, c_{pi} denote the thermal conductivity, density, and specific heat of material i, respectively. Assuming that the temperature perturbation is

$$T(x, y, t) = \mathrm{Re}\{e^{bt+jmx}\Gamma(y)\} \tag{2}$$

where b represents the exponential growth rate, j indicates an imaginary unit, $m = 2\pi/L$ indicates the perturbation frequency, and L is the perturbation wavelength, Γ denotes the nodal temperature vector, which is only related to y and independent of x, the problem is reduced to a one-dimensional system. Substitute Eqs. (2) into (1) and eliminate the exponential terms to obtain

$$K_i \frac{\partial^2 \Gamma}{\partial y^2} - [K_i m^2 + \rho_i c_{pi}(imV + b)]\Gamma = 0 \tag{3}$$

2.1.2 Discretized Governing Equation. Using appropriate boundary conditions and discretizing the model by Galerkin formulation, the resulting equations can be obtained in the matrix form as follows:

$$(\mathbf{S} + V\mathbf{H} + b\mathbf{M})\Gamma + \mathbf{\Phi} f V P = 0 \tag{4}$$

Where

$$\begin{aligned}
\mathbf{S} &= \iint_{\Omega} K_i\left(\frac{\partial \mathbf{W}}{\partial y}\frac{\partial \mathbf{W}^{\mathrm{T}}}{\partial y} + m^2 \mathbf{W}\mathbf{W}^{\mathrm{T}}\right)\mathrm{d}\Omega \\
\mathbf{M} &= \iint_{\Omega} \rho_i c_{pi}\mathbf{W}\mathbf{W}^{\mathrm{T}}\mathrm{d}\Omega \\
\mathbf{H} &= \iint_{\Omega} jm\rho_i c_{pi}\mathbf{W}\mathbf{W}^{\mathrm{T}}\mathrm{d}\Omega \\
\mathbf{\Phi} &= \begin{bmatrix}\mathbf{I}\\ 0\end{bmatrix}_{N\times N_c}
\end{aligned} \tag{5}$$

where Ω indicates the sum of the combined domain of two materials, $\mathbf{W}$ represents a matrix, each row vector of which corresponds to a shape function (i.e., weight function), N and N_c are the number of total nodes and contact nodes, respectively, $\mathbf{I}$ indicates an N_c order identity matrix, P is the vector of the node contact force perpendicular to the contact interface, and f denotes the friction coefficient.

2.1.3 Linear Relation Between P and Γ. The coupling of the contact force with the displacement field and the temperature field

for the thermoelastic contact problem without considering wear can be expressed as

$$\begin{bmatrix}\mathbf{D}_1\\ \mathbf{D}_2\end{bmatrix}U-\begin{bmatrix}\mathbf{G}_1\\ \mathbf{G}_2\end{bmatrix}\Gamma=\mathbf{\Phi}P \tag{6}$$

where U indicates the displacement vector. Considering the Archard Wear Law $u_i^w=\int\omega_i VP\mathrm{d}t$, in which u_i^w and ω_i represent the wear displacement and wear coefficient of material i, respectively, and assuming that wear takes place only on material 1, U needs to be separated into two parts: the part related to the displacement of the contact node, i.e., U_1 and the degrees of freedom of the remaining nodes of the system, i.e., U_2. $\mathbf{D}_1$ and $\mathbf{D}_2$, the coefficient matrix of U, would be therefore divided to $\mathbf{D}_{11}$, $\mathbf{D}_{12}$, and $\mathbf{D}_{21}$, $\mathbf{D}_{22}$, respectively. The contact boundary condition of Eq. (6) can be modified as

$$\begin{bmatrix}\mathbf{D}_{11} & \mathbf{D}_{12}\\ \mathbf{D}_{21} & \mathbf{D}_{22}\end{bmatrix}\begin{bmatrix}U_1-\int\omega_1 VP\mathrm{d}t\\ U_2\end{bmatrix}-\begin{bmatrix}\mathbf{G}_1\\ \mathbf{G}_2\end{bmatrix}\Gamma=\mathbf{\Phi}P \tag{7}$$

The wear problem is related to time t, and the thermoelastic problem is related to the growth rate b. If displacement field, contact pressure field, and temperature field are represented as Ue^{bt}, Pe^{bt}, and Γe^{bt}, the derivative of Eq. (7) with respect to time t can be obtained as

$$\begin{cases}b\mathbf{D}_1U-\mathbf{D}_{11}\omega_1VP-b\mathbf{G}_1\Gamma=bP\\ b\mathbf{D}_2U-\mathbf{D}_{21}\omega_1VP-b\mathbf{G}_2\Gamma=0\end{cases} \tag{8}$$

Combining the two equations and canceling U

$$\mathbf{D}^*VP+b\mathbf{G}^*\Gamma-bP=0 \tag{9}$$

in which

$$\mathbf{D}^*=\omega_1(\mathbf{D}_1\mathbf{D}_2^{-1}\mathbf{D}_{21}-\mathbf{D}_{11}) \tag{10}$$

$$\mathbf{G}^*=\mathbf{D}_1\mathbf{D}_2^{-1}\mathbf{G}_2-\mathbf{G}_1 \tag{11}$$

2.1.4 Eigenvalue Equation. By combining Eqs. (4) and (9), the pressure P gets eliminated and a second-order polynomial eigenvalue equation can be obtained as

$$(b^2\mathbf{Q}_2+b\mathbf{Q}_1-\mathbf{Q}_0)\Gamma=0 \tag{12}$$

Where

$$\mathbf{Q}_0=-\mathbf{D}^*V(\mathbf{S}+V\mathrm{H}) \tag{13}$$

$$\mathbf{Q}_1=(\mathbf{S}+V\mathbf{H})-\mathbf{M}\mathbf{D}^*V-\mathbf{\Phi}fV\mathbf{G}^* \tag{14}$$

$$\mathbf{Q}_2=\mathbf{M} \tag{15}$$

Equation (12) is transformed into two first-order eigenvalue equations to facilitate the solution

$$\left(\begin{bmatrix}\mathbf{Q}_0 & \mathbf{Q}_1\\ \mathbf{O} & \mathbf{I}\end{bmatrix}-b\begin{bmatrix}\mathbf{O} & -\mathbf{Q}_2\\ \mathbf{I} & \mathbf{O}\end{bmatrix}\right)\begin{Bmatrix}\Gamma\\ \tilde{\Gamma}\end{Bmatrix}=0 \tag{16}$$

and

$$\tilde{\Gamma}=b\Gamma \tag{17}$$

The above discussion is based on the assumption that material 2 observes no wear. To investigate the wear of both the materials, $\mathbf{D}^*$ can be redefined as

$$\mathbf{D}^*=\mathbf{D}_1\mathbf{D}_2^{-1}\sum_{i=1}^{2}\mathbf{D}_{21i}\omega_i-\sum_{i=1}^{2}\mathbf{D}_{11i}\omega_i \tag{18}$$

Subscripts $i=1,2$ represent two different materials. The rest of the equation stays the same.

2.2 Analytical Method. The analytical model of wear effects developed by Papangelo and Ciavarella comprises two half-planes with different materials. Relative to the two materials, the disturbance moves on the contact surface, fixed on which is the global coordinate system (x, y). The two materials move at the speed of c_1 and c_2, and the local coordinate system (x_i, y_i) is fixed on them respectively, where i denotes material i $(i=1, 2)$ (as highlighted in Fig. 2). The relative sliding velocity of the two half-planes is $V=|c_1-c_2|$.

2.2.1 Temperature Field. The thermal diffusion equation with the appropriate convection term must be satisfied by the corresponding temperature field T. The transient heat conduction equation is

$$\frac{\partial^2T_i}{\partial x^2}+\frac{\partial^2T_i}{\partial y_i^2}+\frac{c_i}{k_i}\frac{\partial T_i}{\partial x}=\frac{1}{k_i}\frac{\partial T_i}{\partial t} \tag{19}$$

where T_i and $k_i=K_i/\rho_i c_{pi}$ indicate the temperature field and thermal diffusivity of material i and t represent the time. The general solution of the heat conduction equation can be expressed in perturbation form as below:

$$T_i(x_i,y_i,t)=\mathrm{Re}\{\Gamma_0e^{-\lambda_i y_i}e^{bt}e^{jmx}\} \tag{20}$$

where Γ_0 is complex constant, b indicates the perturbation growth rate, and the spatial decay rate of perturbation λ is

$$\lambda_i=\sqrt{m^2+\frac{b}{k_i}-\frac{jmc_i}{k_i}} \tag{21}$$

2.2.2 Pressure Distribution. The displacement on the surface can be caused by three types of deformations: elastic deformation, thermal deformation, and wear deformation. To ensure that the contact surfaces do not separate, the sum of these three displacements of the two materials must be zero

$$\sum_{i=1}^{2}(u_i^{el}+u_i^{th}+u_i^w)=0 \tag{22}$$

where u_i^{el} is the elastic displacement of material i, u_i^{th} represents the thermal displacement of material i, and u_i^w indicates the wear displacement of material i. Displacement and contact pressure are expressed in the form of disturbance to obtain Eq. (23)

$$p_0=\frac{\sum_{i=1}^{2}\dfrac{2\alpha_i(1+\nu_i)}{m+\lambda_i}}{\dfrac{2}{m\tilde{E}}+V\sum_{i=1}^{2}\dfrac{\omega_i}{b-jmc_i}}\Gamma_0 \tag{23}$$

where p_0 indicates the amplitude of pressure disturbance, ω_i represents the wear coefficient of material i, α_i is the thermal expansion coefficient of material i, and $\tilde{E}$ indicates the comprehensive elastic modulus defined as

$$\frac{1}{\tilde{E}}=\frac{1-\nu_1^2}{E_1}+\frac{1-\nu_2^2}{E_2} \tag{24}$$

where E_1, E_2 are Young's elastic modulus, and ν_1, ν_2 are Poisson's ratio of the two materials.

2.2.3 Characteristic Equation. Considering that all the heat generated by the friction goes into the two materials

$$-K_1\frac{\partial T_1}{\partial y_1}-K_2\frac{\partial T_2}{\partial y_2}=fV\mathrm{Re}\{p_0e^{bt}e^{jmx}\} \tag{25}$$

Substituting Eqs. (20) and (23) into Eq. (25) and eliminating the exponential terms, the characteristic equation can be obtained as

$$K_1\lambda_1+K_2\lambda_2=f|c_1-c_2|\times\frac{\dfrac{2\alpha_1(1+\nu_1)}{m+\lambda_1}+\dfrac{2\alpha_2(1+\nu_2)}{m+\lambda_2}}{\dfrac{2}{m\tilde{E}}+|c_1-c_2|\left(\dfrac{\omega_1}{b-jmc_1}+\dfrac{\omega_2}{b-jmc_2}\right)} \tag{26}$$

2.2.4 Dimensionless Formulation. Defining the dimensionless parameters

$$K^* = \frac{K_1}{K_2}, k^* = \frac{k_1}{k_2}, \alpha^* = \frac{\alpha_1(1+\nu_1)}{\alpha_2(1+\nu_2)}$$
$$\lambda_i^* = \frac{\lambda_i}{m}, c_i^* = \frac{c_i}{mk_2}, b^* = \frac{b}{k_2 m^2}$$
$$\omega_i^* = \tilde{E}\omega_i, R^* = \frac{\omega_2}{\omega_1}, H^* = \frac{k_2 f}{K_2}\tilde{E}\alpha_2(1+\nu_2) \quad (27)$$
$$\omega^* = 2H^*, V^* = \frac{2}{H^*}$$

the characteristic Eq. (26) can be restated as follows:

$$(K^*\lambda_1^* + \lambda_2^*)\left[1 + j\frac{\omega_1^*}{2}|c_1^* - c_2^*|\left(\frac{1}{c_1^*} + R^*\frac{1}{c_2^*}\right)\right]$$
$$- H^*|c_1^* - c_2^*|\left(\frac{\alpha^*}{1+\lambda_1^*} + \frac{1}{1+\lambda_2^*}\right) = 0 \quad (28)$$

3 Results and Discussions

To validate the accuracy of the finite element method, the results obtained by the two methods are compared. Figure 3 illustrates the dimensionless critical speed V_{cr}^*/V^* versus the thermal conductivity ratio K^* for $H^* = 0.34$, $R^* = 0.1$, $\alpha^* = 2.5$, and $k^* = K^*$, with different values of wear-rates $\omega_1^*/\omega^* = [0.2, 0.4, 0.6, 0.8, 1]$. The lines in different line styles represent the results obtained by the analytical method, and the marker symbols indicate the results obtained by the finite element method. For $K^* > 0.5$, the critical speed increases with the increase of ω_1^*/ω^*, which means the wear stabilizes the system by inhibiting the TEI. On the contrary, the critical speed reduces with ω_1^*/ω^* for $K^* < 0.5$, which suggests that wear weakens the stability of the system. The two methods lead to results with remarkable consistency, the maximum difference between which is only 1.97%, presenting in an extreme case that the wear coefficient of friction material is equal to the critical values.

Figure 4 demonstrates the dimensionless critical speed V_{cr}^*/V^* versus the dimensionless parameter H^* for $k^* = K^* = 0.1$, and $\alpha^* = 2.5$, with different values of wear-rate $\omega_1^*/\omega^* = [0.1, 0.2, 0.3, 0.4, 0.5]$, and for $R^* = [0.01, 0.05, 0.1]$, respectively, in panels (a), (b), and (c) obtained by the analytical method. The results are almost the same for different ω_1^*/ω^* when $R^* = 0.01$ (Fig. 4(*a*)). With the increase of R^* (Figs. 4(*b*) and 4(*c*)), the differences appear and increase. Moreover, no matter what value of R^* is assumed, the critical velocity increases with the wear-rate ω_1^*/ω^*. The results vary slowly when H^* is large, but with the decrease of H^*, the result changes abruptly. For the commonly used friction

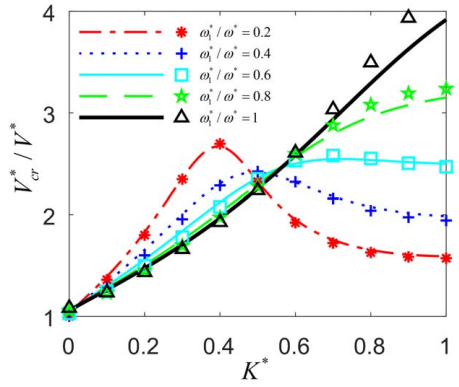

Fig. 3 Dimensionless critical speed V_{cr}^*/V^* versus conductivity ratio K^* for $H^* = 0.34$, $R^* = 0.1$, $\alpha^* = 2.5$, and $k^* = K^*$, with different values of wear-rates $\omega_1^*/\omega^* = [0.2, 0.4, 0.6, 0.8, 1]$

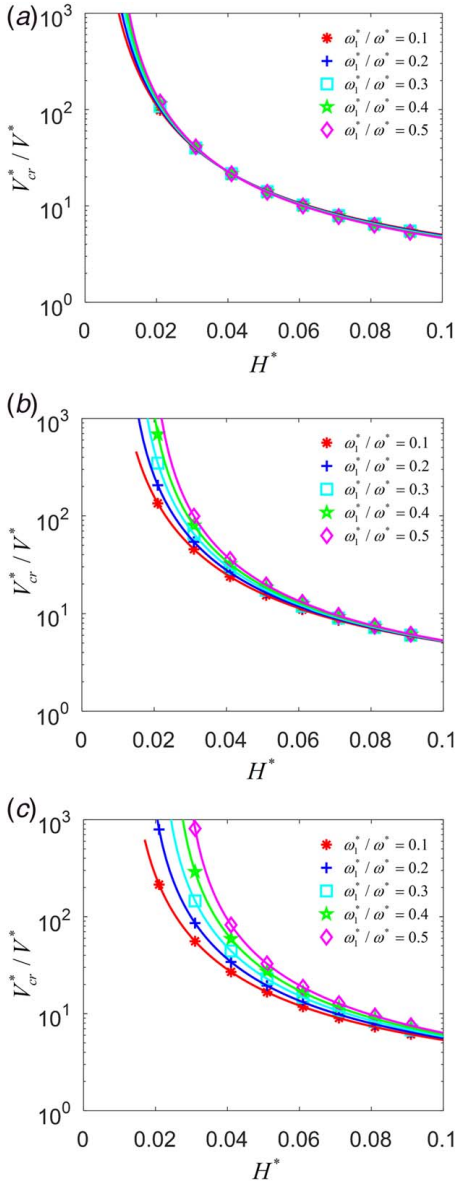

Fig. 4 Dimensionless critical speed V_{cr}^*/V^* versus the dimensionless parameter H^* for $K^* = k^* = 0.1$, $\alpha^* = 2.5$, with different values of wear-rates $\omega_1^*/\omega^* = [0.1, 0.2, 0.3, 0.4, 0.5]$, and for $R^* = [0.01, 0.05, 0.1]$ respectively in panels (*a*), (*b*), and (*c*) obtained by analytical method

pair materials mentioned in Table 1, $H^* = 0.00129$ for the paper-based friction pair and $H^* = 0.00537$ for the Cu-based friction pair. A little change of H^* leads to a magnitude difference of the critical velocity, and the results change too dramatically to converge by the analytical method.

The finite element method can still get convergence solutions when H^* is very small. So, the finite element method can be used to study the influence of wear on TEI more effectively and practically. Figure 5 highlights the dimensionless critical speed V_{cr}^*/V^* as a function of conductivity ratio K^*, with different values of wear-rate ω_1^*/ω^*, for different materials of friction pairs respectively in panels (a) and (b) obtained using finite element method. With the increase of conductivity ratio, the critical velocity increases due to the large unevenness of friction heat distribution between the two materials when the conductivity of the friction material is small and that of the steel material is large. Moreover, the poor internal conductivity of friction material results in a large temperature difference between high- and low-temperature zone in the

Table 1 Material property of the two typical friction pairs used in clutches and brakes [19,20]

	Paper-based pair		Cu-based pair	
	Friction	Steel	Friction	Steel
Young's modulus, E (Pa)	0.53×10^{9}	200×10^{9}	2.26×10^{9}	160×10^{9}
Poisson's ratio, ν	0.3	0.3	0.29	0.29
Density, ρ ($\mathrm{kg\cdot m^{-3}}$)	846	7800	5500	7800
Specific heat, c_p ($\mathrm{J\cdot kg^{-1}\cdot K}$)	4140	449	460	487
Thermal expansion coefficient, α ($\mathrm{K^{-1}}$)	3×10^{-5}	1.2×10^{-5}	1.21×10^{-5}	1.27×10^{-5}
Thermal conductivity, K ($\mathrm{W\cdot m^{-1}\cdot K^{-1}}$)	0.5	42	9.3	45.9

friction material. The possibility of the local high-temperature region in the steel material gets increased due to a large amount of friction heat conducted into the steel material. Due to this, the stability of the system is poor and the critical speed is low for a small conductivity ratio. On the contrary, with the increase of conductivity ratio, the friction heat distribution between the two materials becomes more uniform, the temperature difference between high and low-temperature zone in friction material reduces, and the possibility of high-temperature zone in the steel material reduces. Also, the dimensionless critical speed decreases as the dimensionless friction material wear-rate increases, on the ground that the greater the wear-rate of friction material, the faster the reduction of friction material thickness; the smaller the remaining thickness, the larger the internal temperature gradient and the smaller the heat capacity of the friction material, the more friction heat into the steel material, the more uneven the distribution of friction heat between the two materials, the worse the thermoelastic stability of the system. It is worth noticing that the limit wear coefficient W_{lim}^{NC} obtained by Papanglo and Ciavarella [16,17], above which the TEI is eliminated, is not obtained using the finite element method. This suggests that the critical velocity can still be obtained after the wear coefficient of friction material ω_1 exceeds W_{lim}^{NC}. As represented in Fig. 5, when $\omega_1/W_{\mathrm{lim}}^{NC}=\omega_1^*/\omega^*\geq 1$, the critical velocity is not infinite. This is because the finite element method uses a finite thickness model, while the analytical method uses a semi-infinite thickness model. As for the materials listed in Table 1, $W_{\mathrm{lim}}^{NC}=4.45\times10^{-12}$ [1/Pa] for paper-based pair and $W_{\mathrm{lim}}^{NC}=4.31\times10^{-12}$ [1/Pa] for Cu-based pair, which are from two to three orders of magnitude higher than the typical wear-rates $1\sim20\times10^{-14}$ [1/Pa]. The resulting curve at the typical wear-rate is indistinguishable from the curve $\omega_1^*/\omega^*=0.1$ (also refer to Figs. 6 and 7).

The friction material thickness greatly affects the critical velocity. Figure 6(*a*) demonstrates the critical velocity V_{cr} versus friction material thickness a_1 for the conductivity ratio $K^*=0.01$, steel material wear-rate $\omega_2^*/\omega^*=0.1$, and steel material thickness $a_2=0.5$ m, at different wear coefficient ratios $R^*=[1,\ 0.01,\ 0.002,\ 0.001]$. The critical velocity remains the same with the thickness of the friction material when the friction material thickness $a_1\geq0.2$ m, where the friction material is approximately semi-infinite plane and the thickness has negligible effect on the

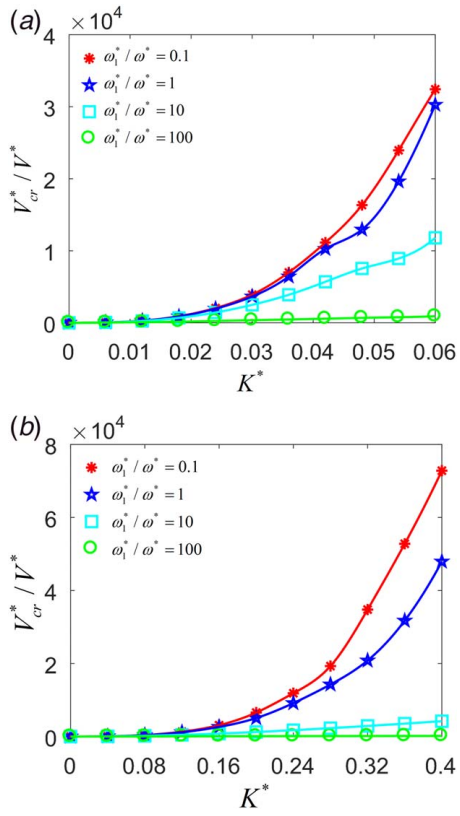

Fig. 5 Dimensionless critical speed V_{cr}^*/V^* as a function of conductivity ratio K^*, for $R^*=0.1$ with different values of wear-rates $\omega_1^*/\omega^*=[0.1,1,10,100]$ obtained by finite element method: (*a*) paper-based friction pairs and (*b*) Cu-based friction pairs

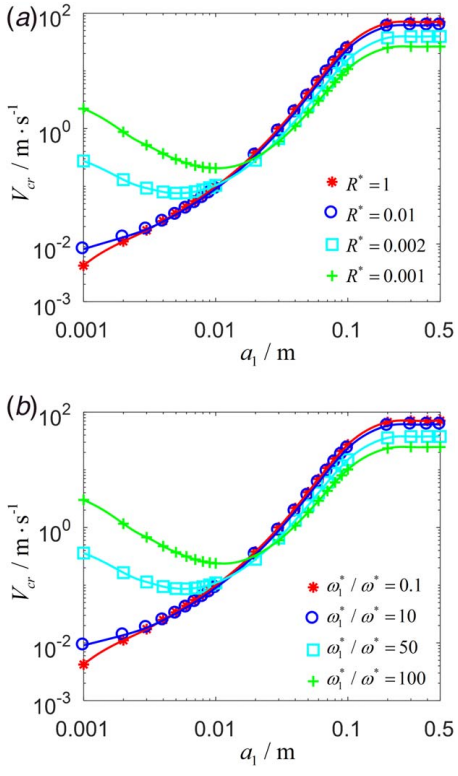

Fig. 6 Critical velocity V_{cr} versus friction material thickness a_1 for conductivity ratio $K^*=0.01$, steel material thickness $a_2=0.5$ m: (*a*) for steel material wear-rate $\omega_2^*/\omega^*=0.1$, at different wear coefficient ratios $R^*=[1,\ 0.01,\ 0.002,\ 0.001]$ and (*b*) for wear coefficient ratio $R^*=0.1$, at different friction material wear-rates $\omega_1^*/\omega^*=[0.1,\ 10,\ 50,100]$

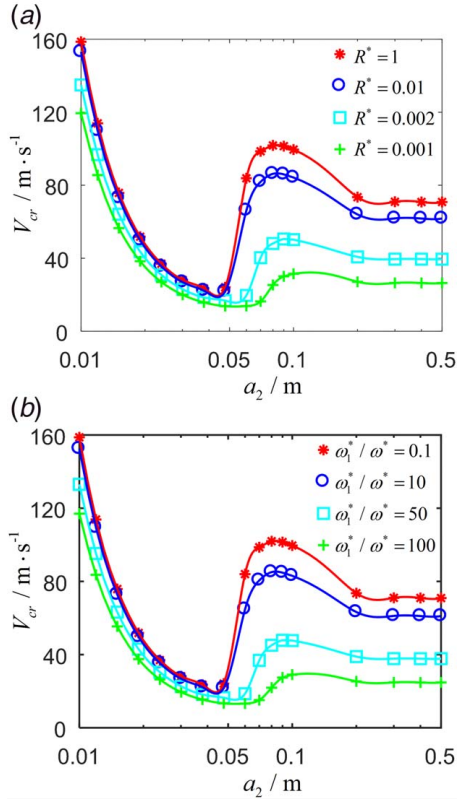

Fig. 7 Critical velocity V_{cr} versus steel material thickness a_2 for conductivity ratio $K^* = 0.01$, friction material thickness $a_1 = 0.5$m: (*a*) for steel material wear-rate $\omega_2^*/\omega^* = 0.1$, at different wear coefficient ratios $R^* = [1, 0.01, 0.002, 0.001]$ and (*b*) for wear coefficient ratio $R^* = 0.1$, at different friction material wear-rates $\omega_1^*/\omega^* = [0.1, 10, 50, 100]$

thermoelastic instability. For the friction material thickness $0.02\,\text{m} \le a_1 \le 0.1\,\text{m}$, the critical velocity is positively correlated with the thickness of the friction material. This is because the internal temperature gradient decreases and the heat capacity increases with the increase of the friction material thickness. Also, the friction heat entering the steel material decreases, enhancing the thermoelastic stability of the system. The critical speed decreases with the increase of friction material thickness, when the friction material thickness $a_1 \le 0.01\,\text{m}$ and the wear coefficient ratio $R^* \subset [0.001, 0.002]$. This is because the wear-rate of the friction material is larger at the same relative sliding friction velocity when the wear coefficient ratio is relatively smaller. Thus, the friction material is lost more, and the remaining friction material is less. The internal temperature gradient of friction material increases and the heat capacity decreases, the temperature rising rate increases, and the heat is distributed less evenly between the two materials, so the thermoelastic stability of the system is worse. When the friction material thickness $a_1 \le 0.01\,\text{m}$ and the wear coefficient ratio $R^* \subset [0.01, 1]$, the critical speed increases with the increase of friction material thickness. This is due to the smaller wear-rate of the friction material for relatively larger wear coefficient ratio. Thus, the lost amount of friction material is not very high, and the dominant factors are still the internal temperature gradient and the heat capacity. The relationship of critical speed with friction material thickness is the same as when $0.01\,\text{m} \le a_1 \le 0.1\,\text{m}$. Figure 6(*a*) also highlights that the critical velocity increases with the increase of the wear coefficient ratio R^* when the friction material thickness is $a_1 > 0.02\,\text{m}$. This is because the greater the wear coefficient ratio, the smaller the friction material wear-rate. The slower the friction material reduces, the smaller the internal temperature gradient and the greater the heat capacity of friction material. The less the friction heat into steel material, the more evenly the friction heat is distributed between the two materials, the better the thermoelastic stability of the system. On the contrary, the critical velocity reduces with the increase of the wear coefficient ratio R^* when the friction material thickness $a_1 < 0.01\,\text{m}$. This is because the more the remaining friction material, the smaller the thermoelastic deformation of the friction material, the greater the internal thermoelastic stress, and the weaker the thermoelastic stability of the system.

Figure 6(*b*) illustrates the critical velocity V_{cr} versus friction material thickness a_1 for conductivity ratio $K^* = 0.01$, wear coefficient ratio $R^* = 0.1$, and steel material thickness $a_2 = 0.5\,\text{m}$, at different wear-rates $\omega_1^*/\omega^* = [0.1, 10, 50, 100]$. It can be observed that the change rule of the critical velocity relative to the thickness of the friction material is the same as that in Fig. 6(*a*). This is because the wear-rate of the friction material plays a significant role in the thermoelastic instability of the system. On the other hand, the thermoelastic instability of the system is also affected by the wear-rate of the steel material. For example, the curve $R^* = 0.002$ in Fig. 6(*a*) has the same wear-rate of the frictional material as the curve $\omega_1^*/\omega^* = 50$ in Fig. 6(*b*), identified as Curve 1 and Curve 2, respectively. The difference is the steel material wear-rate $\omega_2^*/\omega^* = 0.1$ of Curve 1, while $\omega_2^*/\omega^* = 5$ of Curve 2. When the thickness of friction material is $a_1 = 0.5\,\text{m}$, the critical velocity of Curve 1 is 39.4922 m/s, and the critical velocity of Curve 2 is 37.7539 m/s. In this case, the critical velocity reduces with the increase of the wear-rate of steel material. This is because the larger the steel material wear-rate, the less the remaining steel material at the same relative slide velocity, the smaller the heat capacity of the steel material, the faster the temperature rises, the larger the internal temperature gradient, the worse the thermoelastic stability of the system. For $a_1 = 0.01\,\text{m}$, the critical velocities of Curve 1 and Curve 2 are 0.1039 m/s and 0.1096 m/s, respectively; for $a_1 = 0.001\,\text{m}$, the critical velocity of Curve 1 and Curve 2 are 0.2754 m/s and 0.3601 m/s, respectively. The critical velocities increase with the increase of the wear-rate of the steel material. This is because the larger the steel material wear-rate, the less the remaining steel material, the larger the thermoelastic deformation and the smaller the internal thermoelastic stress of the steel material under the same temperature field and contact pressure, thus the higher the thermoelastic stability of the system.

The thickness of steel material also significantly affects the critical velocity. Figure 7(*a*) highlights the critical velocity V_{cr} versus steel material thickness a_2 for conductivity ratio $K^* = 0.01$, steel material wear-rate $\omega_2^*/\omega^* = 0.1$, and friction material thickness $a_1 = 0.5\,\text{m}$, at different wear coefficient ratios $R^* = [1, 0.01, 0.002, 0.001]$. The critical velocity remains constant with the thickness of the steel material when the steel material thickness $a_2 \ge 0.2\,\text{m}$. In that case, the steel material is approximately a semi-infinite plane, and the thickness has a negligible effect on the thermoelastic instability. When the thickness of the steel material is $0.06\,\text{m} < a_2 < 0.2\,\text{m}$, the relationship between the critical velocity and the thickness of the steel material is in an anti-parabolic shape. This means that with the decrease of the steel material thickness, the critical velocity first increases and then drops. Regardless of the wear coefficient ratio, there is a local maximum critical velocity to which the corresponding thickness is defined as the *local optimum thickness*. When the thickness of the steel material decreases below the local optimum thickness, the critical velocity reaches the minimum value, to which the corresponding thickness of the steel material is defined as the *worst thickness*. Two factors account for this phenomenon: (1) The thermoelastic deformation of the steel material increases with the decrease of the steel material thickness, and the internal thermoelastic stress decreases under the action of the same temperature field and contact pressure. This increases the thermoelastic stability of the system. (2) With the decrease of the steel material thickness, the internal temperature gradient increases, and the heat capacity reduces, the temperature rising rate increases, so the thermoelastic stability of the system decreases. When the thickness of the steel material is greater than the local optimum thickness or smaller than the local worst thickness, factor (1) plays a leading role. On the contrary, when the thickness of the steel material is less than the local

optimum thickness and greater than the local worst thickness, factor (2) plays a key role. The local optimal thickness is a little larger for the current commonly used clutch and brake. This is due to the structural limitations of the components, and it is more convenient to enhance the thermoelastic stability by decreasing the thickness of the steel material. However, it must be noted that clutches or brakes with steel material thickness between 30 mm and 110 mm will appear in the future, the structural design and optimization of which will require the results of this paper to make the thickness of steel material close to the local optimum thickness and also to avoid the worst thickness. Figure 7(*a*) also indicates that, regardless of the thickness of the steel material, critical velocity increases with the increase of the wear coefficient ratio. In particular, the local maximum critical velocity increases the most and the corresponding local optimal thickness increases accordingly. Considering that the greater the wear coefficient ratio, the smaller the friction material wear-rate, as the steel material wear-rate is constant, the slower the friction material thickness, the more the remaining friction material, the smaller the internal temperature gradient, the greater the heat capacity, the less friction heat into the steel material, the more evenly the friction heat is distributed between the two materials, thus the stronger the thermoelastic stability of the system.

Figure 7(*b*) highlights the critical velocity V_{cr} versus steel material thickness a_2 for conductivity ratio $K^* = 0.01$, wear coefficient ratio $R^* = 0.1$, and friction material thickness $a_1 = 0.5$ m, at different wear-rates $\omega_1^*/\omega^* = [0.1, 10, 50, 100]$. It can be observed that the change rule of the critical velocity relative to the thickness of the steel material is the same as that in Fig. 7(*a*) because the wear-rate of the friction material plays a key role in the thermoelastic stability of the system. Besides, the wear-rate of the steel material also affects the thermoelastic instability of the system. For instance, the curve $R^* = 1$ in Fig. 7(*a*) has the same wear-rate of the frictional material as the curve $\omega_1^*/\omega^* = 0.1$ in Fig. 7(*b*), identified as Curve 3 and Curve 4, respectively. The difference is the steel material wear-rate $\omega_2^*/\omega^* = 0.1$ of Curve 3, while $\omega_2^*/\omega^* = 0.01$ of Curve 4. Regardless of the steel material thickness, the critical speed of Curve 4 is greater than that of Curve 3. This is because the larger the steel material wear-rate, the smaller the remaining steel material, the larger the internal temperature gradient, the smaller the heat capacity, and the faster the temperature rise rate, thus the lower the thermoelastic stability of the system.

4 Conclusions

Thermoelastic instability proves to be the root cause of hotspots in clutches and brakes. The study of the comprehensive effect of wear and friction pair thickness on TEI must be conducted for the structure optimization of friction pairs, the selection of friction materials, and the improvement of thermoelastic stability. Although it is difficult to solve the TEI problem of the friction pair used in conventional clutch and brake systems using the analytical method, the finite element method provides a better approach to efficiently figure out the effects of the wear coefficient and the thickness of the friction pair (including friction material and steel material) on the critical speed of TEI.

When the thickness of friction material is below 10 mm, TEI is inhibited by wear, and conversely, it gets promoted by wear. For the small wear-rate of friction material, the increase of friction material thickness will suppress the TEI; for the large wear-rate of friction material, the increase of friction material thickness first promotes and then inhibits the TEI.

The local optimum thickness and the worst thickness are observed in the steel material, and the worst steel thickness must be avoided in the design. In practical engineering applications, the impact of steel wear-rate on TEI is complex yet inconspicuous and could be ignored compared to the wear of friction materials. In the future, the existing two-dimensional model can be extended to a three-dimensional axisymmetric model to provide more accurate predictions.

Acknowledgment

The idea of implementing the finite element method to study the effect of wear in thermoelastic instability originated from the discussion and communication between the authors and Professor Yong Hoon Jang at Yonsei University, Korea. We gratefully acknowledge Professor Jang's contribution and pioneering work in this area. Support for this work, provided by Open Foundation of The State Key Laboratory of Mechanical Transmissions (SKLMT-MSKFKT-202004), the National Science Foundation under Contract (Grant No. 1928876), and National Natural Science Foundation of China (Grant Nos. 51805351 and U1810123), is also gratefully acknowledged.

Conflict of Interest

There are no conflicts of interest.

Data Availability Statement

The data sets generated and supporting the findings of this article are obtainable from the corresponding author upon reasonable request. The authors attest that all data for this study are included in the paper. Data provided by a third party are listed in Acknowledgment. No data, models, or code were generated or used for this paper.

Nomenclature

j = imaginary unit
k = thermal diffusivity
m = perturbation frequency
t = time
x = slip direction
y = thickness direction
$\mathbf{M}$ = mass matrix
$\mathbf{O}$ = identity matrix
$\mathbf{S}$ = conductivity matrix
K = thermal conductivity
L = perturbation wavelength
N = number of total nodes
P = vector of the node contact force
T = temperature field
U = displacement vector
V = relative speed
k^* = thermal diffusivity ratio
K^* = thermal conductivity ratio
R^* = wear coefficient ratio
V^* = dimensionless Burton critical speed
p_0 = amplitude of pressure disturbance
N_c = number of contact nodes
U_1 = contact nodes displacement
U_2 = remaining node displacement
V_{cr} = critical speed
u_i^{el} = elastic displacement of material i
u_i^{th} = thermal displacement of material i
u_i^{w} = wear displacement of material i
V_{cr}^* = dimensionless critical speed
$\mathbf{Q}_0$, $\mathbf{Q}_1$, $\mathbf{Q}_2$ = coefficient matrix of eigenvalue equation
α^* = thermal expansion coefficient ratio
α_i = thermal expansion coefficient of material i
Γ = vector of the node temperature
$\tilde{\Gamma}$ = facilitating vector
Γ_0 = complex constant
λ_i = spatial decay rate of material i
λ_i^* = dimensionless spatial decay rate of material i
ν_i = Poisson's ratio of material i
ρ_i = density of material i
Φ = coefficient matrix

ω_i = wear coefficient of material i
ω^* = critical wear coefficient
ω_i^* = dimensionless wear coefficient of material i

References

[1] Cui, H. W., Wang, Q. L., Lian, Z. S., and Li, L., 2019, "Theoretical Model and Experimental Research on Friction and Torque Characteristics of Hydro-viscous Drive in Mixed Friction Stage," Chin. J. Mech. Eng., **32**(80), pp. 1–11.

[2] Wang, Q. L., Cui, H. W., Lian, Z. S., and Li, L., 2019, "Thermoelastic Analysis of Friction Pairs in Hydro-viscous Drive Combined Thermal and Mechanical Loads Under Soft Startup Condition," Numer. Heat Transfer, Part A, **75**(5), pp. 327–341.

[3] Hartsock, D. L., and Fash, J. W., 2000, "Effect of Pad/Caliper Stiffness, Pad Thickness, and Pad Length on Thermoelastic Instability in Disk Brakes," ASME J. Tribol., **122**(3), pp. 511–518.

[4] Barber, J. R., 1969, "Thermoelastic Instabilities in the Sliding of Conforming Solids," Proc. R. Soc. London, Ser. A, **312**(1510), pp. 381–394.

[5] Lee, K., and Barber, J. R., 1993, "Frictionally Excited Thermoelastic Instability in Automotive Disk Brakes," ASME J. Tribol., **115**(4), pp. 607–614.

[6] Dow, T. A., and Burton, R. A., 1972, "Thermoelastic Instability of Sliding Contact in the Absence of Wear," Wear, **19**(3), pp. 315–328.

[7] Burton, R. A., Nerlikar, V., and Kilaparti, S. R., 1973, "Thermoelastic Instability in a Seal-Like Configuration," Wear, **24**(2), pp. 177–188.

[8] Jang, J. Y., and Khonsari, M. M., 2004, "On the Growth Rate of Thermoelastic Instability," ASME J. Tribol., **126**(1), pp. 50–55.

[9] Yi, Y. B., Barber, J. R., and Zagrodzki, P., 2000, "Eigenvalue Solution of Thermoelastic Instability Problems Using Fourier Reduction," Proc. R. Soc. London, Ser. A, **456**(2003), pp. 2799–2821.

[10] Yi, Y. B., 2006, "Finite Element Analysis of Thermoelastodynamic Instability Involving Frictional Heating," ASME J. Tribol., **128**(4), pp. 718–724.

[11] Mortazavi, V., Wang, C. F., and Nosonovsky, M., 2012, "Stability of Frictional Sliding With the Coefficient of Friction Depended on the Temperature," ASME J. Tribol., **134**(4), p. 041601.

[12] Zagrodzki, P., Lam, K. B., Al-Bahkali, E., and Barber, J. R., 2001, "Nonlinear Transient Behavior of a Sliding System With Frictionally Excited Thermoelastic Instability," ASME J. Tribol., **123**(4), pp. 699–708.

[13] Zagrodzki, P., 2009, "Thermoelastic Instability in Friction Clutches and Brakes-Transient Modal Analysis Revealing Mechanisms of Excitation of Unstable Modes," Int. J. Solids Struct., **46**(11–12), pp. 2463–2476.

[14] Al-Shabibi, A. M., 2014, "Transient Behavior of Initial Perturbation in Multidisk Clutch System," Tribol. Trans., **57**(6), pp. 1164–1171.

[15] Dow, T. A., and Burton, R. A., 1973, "The Role of Wear in the Initiation of Thermoelastic Instabilities of Rubbing Contact," ASME J. Lubr. Technol., **95**(1), pp. 71–75.

[16] Papangelo, A., and Ciavarella, M., 2020, "Can Wear Completely Suppress Thermoelastic Instabilities?," ASME J. Tribol., **142**(5), p. 051501.

[17] Papangelo, A., and Ciavarella, M., 2020, "The Effect of Wear on Thermoelastic Instabilities (TEI) in Bimaterial Interfaces," Tribol. Int., **142**, p. 105977.

[18] Qiao, Y. J., Ciavarella, M., Yi, Y. B., and Wang, T., 2020, "Effect of Wear on Frictionally Excited Thermoelastic Instability: A Finite Element Approach," J. Therm. Stresses, **43**(12), pp. 1564–1576.

[19] Koranteng, K., Shaahu, J. S., Ma, C. N., Li, H. Y., and Yi, Y. B., 2021, "The Performance of Cu-Based Friction Material in Dry Clutch Engagement," Proc. Inst. Mech. Eng. J-J. Eng. Tribol., **235**(6), pp. 1114–1123.

[20] Zhao, J. X., 2014, "Research on Thermoelastic Instability of Shifting Clutches in the Process of Engagement," Ph.D. dissertation, Beijing Institute of Technology, Beijing.